

Memristor Effect on Bundles of Vertically Aligned Carbon Nanotubes Tested by Scanning Tunnel Microscopy

O. A. Ageev*, Yu. F. Blinov, O. I. Il'in, A. S. Kolomiitsev, B. G. Konoplev,
M. V. Rubashkina, V. A. Smirnov, and A. A. Fedotov

Southern Federal University, Nekrasovskii per. 44, Taganrog, 347928 Russia

**e-mail: ageev@sfedu.ru*

Received February 27, 2013

Abstract—We report on the results of experimental study of an array of vertically aligned carbon nanotubes (VA CNTs) by scanning tunnel microscopy (STM). It is shown that upon the application of an external electric field to the STM probe/VA CNT system, individual VA CNTs are combined into bundles whose diameter depends on the radius of the tip of the STM probe. The memristor effect in VA CNTs is detected. For the VA CNT array under investigation, the resistivity ratio in the low- and high-resistance states at a voltage of 180 mV is 28. The results can be used in the development of structures and technological processes for designing nanoelectronics devices based on VA CNT arrays, including elements of ultrahigh-access memory cells for vacuum microelectronics devices.

DOI: 10.1134/S1063784213120025

INTRODUCTION

The development and testing of energy-independent high-access memory elements is one of the priority trends in the development of contemporary nanoelectronics [1]. A perspective element of such random access memory is a memristor, viz., a bistable element whose resistance changes upon the application of an external field [2, 3]. A typical feature of the memristor is its ability to preserve the value of the resistance after the removal of the external field.

Carbon nanotubes (CNTs) belong to the promising class of nanomaterials possessing unique properties. In particular, vertically aligned carbon nanotubes (VA CNTs) [4, 5] can be used in designing new devices in nano- and microelectronics. The observation of the memristor effect on monolayer semiconductor CNTs aligned horizontally on a substrate and on gold-modified misaligned CNTs was reported in [6] and [7], respectively. However, the memristor effect in both cases was associated not only with the properties of nanotubes themselves, but with additional imposed conditions also. For example, the memristor effect in [6] was induced by the interaction of a nanotube with an insulating substrate and in [7], by the presence of gold nanoislands on the CNT surface. The possibility of a manifestation of the memristor effect due to the properties of CNTs themselves has been investigated insufficiently.

Scanning tunnel microscopy (STM) is a precision method for analyzing the properties of nanomaterials and nanostructures [8, 9]. The STM method is contact-free and makes it possible to study the properties of vertically aligned CNTs with a high resolution,

which cannot be achieved using other methods (in particular, atomic force microscopy) in view of the high mobility of VA CNTs during the interaction of the probe with their surface [10, 11].

This work is aimed at analysis of the features of interaction of a STM probe with the surface of the VA CNT array based on the STM method.

1. EXPERIMENTAL

As the experimental sample, we used a VA CNT array grown by plasma-enhanced chemical vapor deposition (PECVD) from the gas phase at the multifunctional complex NANOFAB NTK-9 (NT-MDT, Russia). As the substrate, we used a silicon plate with a bilayer structure consisting of a 20-nm-thick titanium film and a 10-nm-thick nickel film formed on its surface. The reaction gas was acetylene. The regimes of VA CNT growth are described in greater detail in [4, 5].

The geometrical parameters of the VA CNT array (diameter, height, CNT number density in the array) were estimated preliminarily using the Nova NanoLab 600 scanning electron microscope (FEI, the Netherlands).

The surface of the VA CNT array was studied experimentally in the dc regime at a voltage $U = 0.1$ V using the Solver P47 Pro scanning probe microscope (NT-MDT, Russia). The role of the lower electrode in the VA CNT was played by the conducting layer formed on the silicon substrate surface after the growth of the CNT, while the upper electrode was the tungsten STM probe sharpened by electrochemical etching; we used two STM probes with different radii

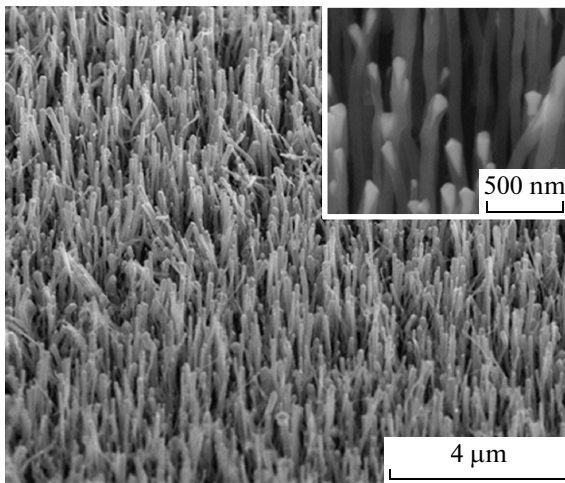


Fig. 1. SEM images of the experimental sample with a VA CNT array under a magnification of 200 000 \times ; the inset shows the SEM image under a magnification of 160 000 \times .

of the tip. The geometrical parameters of the VA CNT array were determined by statistical processing of the resultant STM images using the Image Analysis 3.5 software package (NT-MDT, Russia).

2. RESULTS AND DISCUSSION

Analysis of the scanning electron microscope (SEM) images (Fig. 1) shows that average VA CNT diameter D is about 95 nm, the average CNT height L is about 1 μm , and the average number density m in the array is about 30 μm^{-2} . The growth of VA CNTs followed the vertex mechanism (see inset to Fig. 1); at the vertex of each VA CNT, a catalytic nickel center in the form of a cone with a base diameter of about 95 nm and an average height above the VA CNT surface of about 28 nm was located.

SEM analysis of STM probes (Figs. 2a, 2c) made it possible to determine the radii of the probes (146 and 50 nm). The current—height characteristics (Figs. 2b, 2d) obtained in the STM-spectroscopy regime using the prepared STM probes show that the effective probe radius is 2.0 and 0.5 nm, respectively.

Analysis of the resultant STM images of the VA CNT array (Fig. 3) revealed that individual VA CNTs are combined into bundles under the action of an STM probe.

Experimental studies of the effect of the CNT-probe tip radius on the diameter of VA CNT bundles formed has shown that a decrease in the tip radius reduces the VA CNT diameter due to a decrease in the area of the region of action of the field produced by the STM probe. For example, when the VA CNT array is scanned by a STM probe with a tip radius of 146 nm, the bundle diameter was 1194 nm (Figs. 3a, 3b), while the bundle diameter for STM probes with a radius of 50 nm was 436 nm (Figs. 3c, 3d).

Another feature of the interaction of the STM probe with the surface of an array of VA CNTs is that the average height of the CNT bundles determined by the STM method (Figs. 3b, 3d) is much smaller than the VA CNT height obtained by the SEM method. This can be due to the limited depth of penetration of the STM probe between the bundles during dc scanning (Fig. 4a). The revealed features must be taken into account in analysis of STM images of the VA CNT array surface.

The process of bunching of individual VA CNTs can be associated with the action of electric forces emerging in the STM-probe/VA CNT-array systems under the action of a nonuniform external electric field. Analysis has shown that the main contribution to VA CNT bunching comes from the surface force of attraction between the STM probe and the nanotube, which is directed towards the region of the highest field strength (Fig. 4b):

$$F_{\text{at}} = 0.5\varepsilon\varepsilon_0 E^2 S, \quad (1)$$

where ε is the CNT permittivity, S is the CNT cross-sectional area, and E is the field strength. When the distance between the probe and the sample is 0.5 nm, the probe tip radius is 50 nm, and the applied voltage is 0.1 V, the field strength is 2×10^8 V/m, and the corresponding attractive force is $F_{\text{at}} = 78.5$ nN. The surface attractive force between the VA CNT and the STM probe can emerge due to the longitudinal polarization of the VA CNT by the external electric field [12, 13].

The action of the attractive force leads to the emergence of the elastic force opposing it:

$$F_{\text{at}} = -F_{\text{el}} = k\Delta L, \quad (2)$$

where ΔL is the VA CNT elongation, k is the elastic modulus ($k \approx 0.15 YD^4/L^3$ [14]), Y is the VA CNT elastic modulus, and D and L are the VA CNT diameter and height, respectively. The Young modulus of the VA CNTs under investigation was determined using the technique developed earlier [10] and was $Y = 1.33 \pm 0.07$ TPa. The average diameter and height of the VA CNTs were determined using the SEM and STM images and were found to be $D = 95$ nm and $L = 1$ μm .

Estimates show that the emerging attractive force leads to the nanotube elongation $\Delta L = 65$ nm (which amounts to approximately 6% of the VA CNT height). When the STM probe is displaced, the CNT is deflected along the scanning line. For a high density of the VA CNT array (of about 30 μm^{-2}), a deflection of a few nanometers is sufficient for an adjacent VA CNT to get into the zone of field action and to be combined with the previous nanotube.

Analysis of the mechanical stresses emerging in the VA CNT bundle under the action of the attractive force upon a displacement of the STM probe along the scanning line shows that the force retrieving the nanotube to the initial position is $F_x = F_y \cot \beta = F_{\text{at}} \cot \beta$, where β is the angle of VA CNT inclination to the sub-

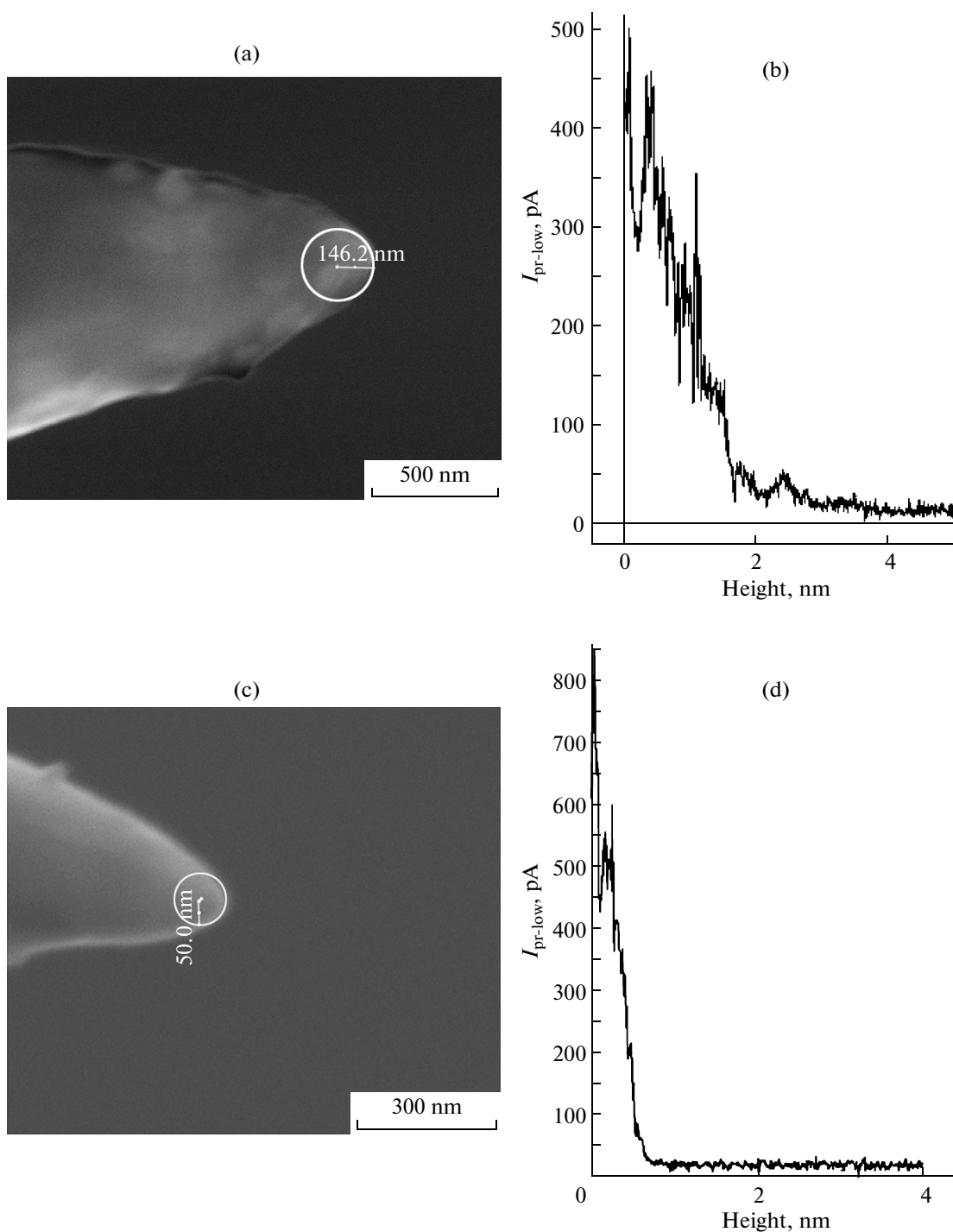


Fig. 2. SEM images of tungsten probes and corresponding current–height characteristics: (a, b) probe with a tip radius of 146 nm and an effective radius of 2 nm; (c, d) probe with a tip radius of 50 nm and an effective radius of 0.5 nm.

strate (see Fig. 4b). Consequently, for $\beta > 45^\circ$, we have $F_{at} > F_x$ ($\cot\beta < 1$), and the nanotube remains in the field of action of attractive forces; for smaller inclination angles ($\cot\beta > 1$, $F_x > F_{at}$), the nanotube returns to its initial position. Consequently, the maximal deviation of the VA CNT under the action of surface attractive forces when the VA CNT is inclined directly from the base is given by

$$x_{\max} = L \cos 45^\circ. \quad (3)$$

The results of experimental investigations of the VA CNT array show that the CNTs forming bundles have an angle of inclination to the substrate exceeding 45° (Figs. 3b, 3d).

After the removal of the external field, the VA CNT bundles do not disintegrate into individual tubes prob-

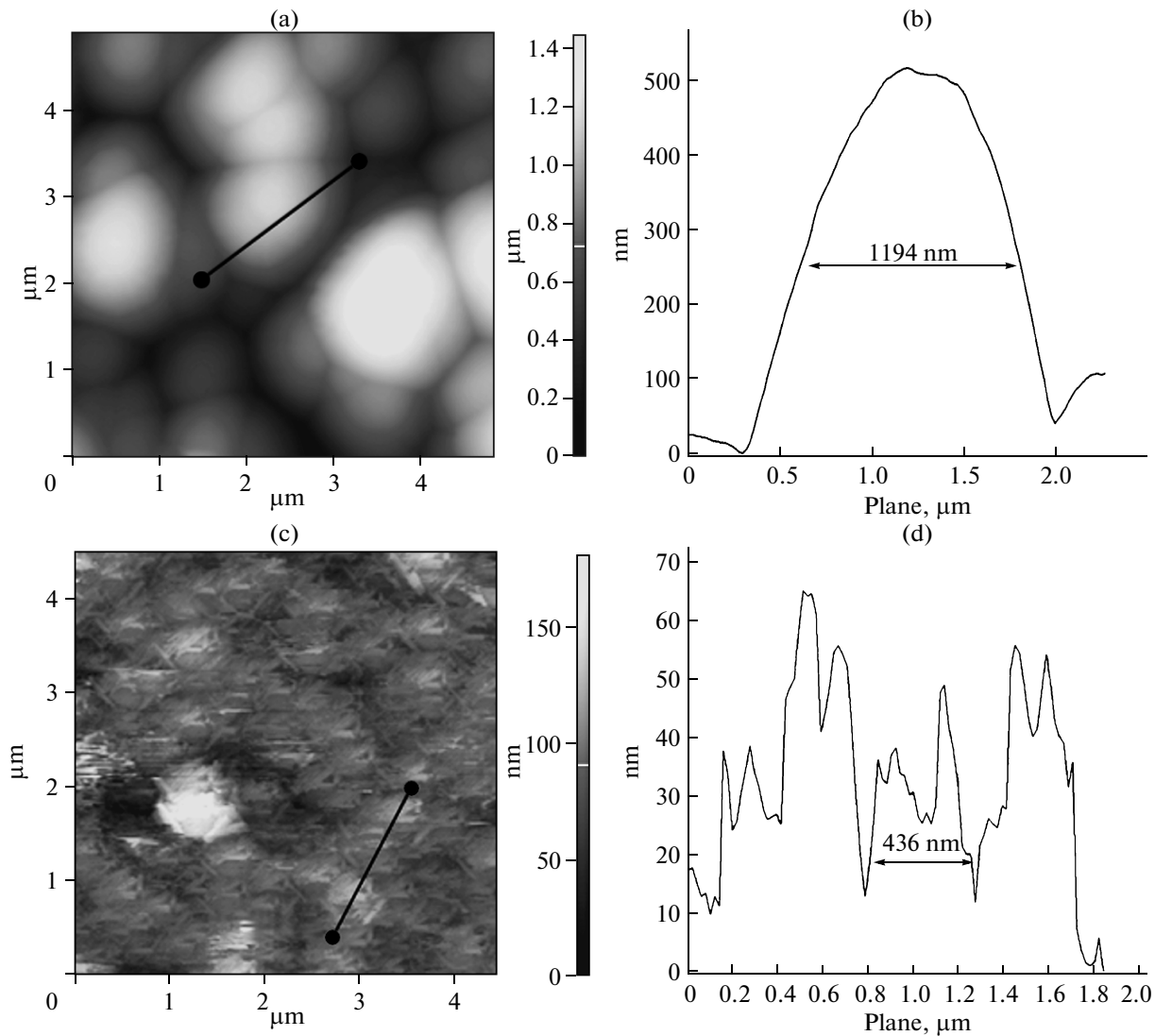


Fig. 3. Results of analysis of the VA CNT method by the STM method: (a) STM image and (b) cross section profile obtained with a probe having a tip radius of 146 nm; (c) STM image and (d) cross section profile obtained with a probe having a tip radius of 50 nm.

ably as a result of action of the van der Waals forces emerging between CNTs during the formation of a VA CNT bundle. The van der Waals force acting between two carbon atoms is given by

$$F_{\text{vdw}C-C} = -\frac{dW}{dr} = -\frac{d}{dr} \left(\frac{3 J_c J_c \alpha_c^2}{2(J_c + J_c) r^6} \right) = \frac{9 J_c \alpha_c^2}{2 r^7}, \quad (4)$$

where J_c is the ionization potential, α_c is the polarizability, and r is the atomic spacing.

Then, the force of interaction between VA CNT vertices is

$$F_{\text{vdw}} = \frac{9 J_c \alpha_c^2 N}{2 r^7}, \quad (5)$$

where N is the number of carbon atoms participating in the interaction. Preliminary estimation has shown

that the van der Waals attractive forces acting between the VA CNT vertices amount to $F_{\text{vdw}} = 50 \mu\text{N}$ for a distance of 0.5 nm between the vertices and considerably exceed the maximal force tending to retrieve the nanotube to its initial position ($(F_x)_{\text{max}} = F_{\text{at}}$). Analogous calculations for nickel atoms have shown that the van der Waals attractive forces acting between nickel particles at the tips of a VA CNT amount to $F_{\text{vdw}} = 16 \mu\text{N}$. After the removal of the external electric field, the CNTs remain in the stressed state; as a result, the geometrical shape of the VA CNT bundle is preserved.

Experiments show that the bunching of VA CNTs is observed for the negative as well as positive polarity of the probe, which is in conformity with the proposed mechanism of combining individual nanotubes into VA CNT bundles.

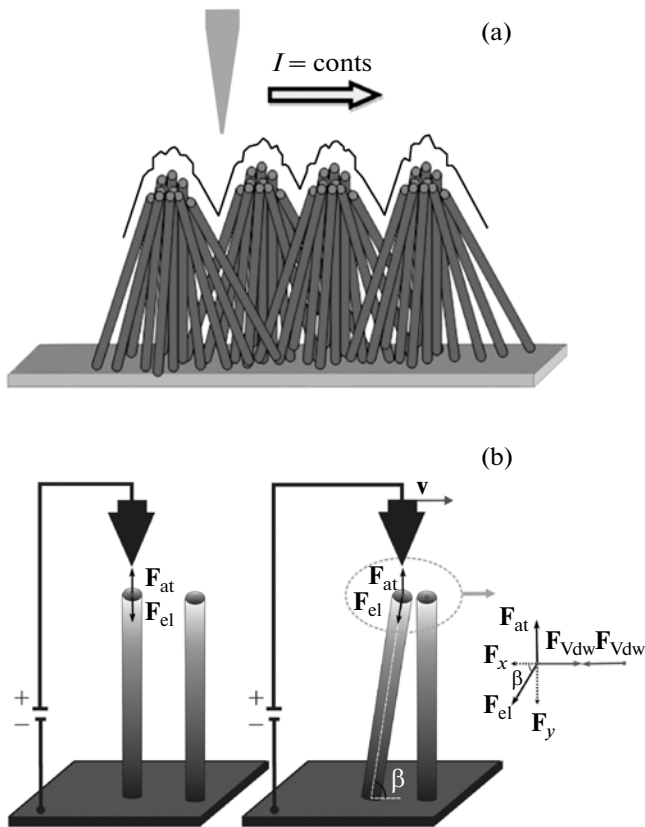


Fig. 4. Schematic diagram of processes of (a) formation of the STM image and (b) interaction of the VA CNT with the STM probe under the action of the external field.

Analysis of a VA CNT array by an STM probe with a tip radius of 50 nm (see Fig. 3c) in the STM-spectroscopy regime has shown that the current–voltage (I – V) characteristics obtained during investigation of the tip of the VA CNT bundle by an STM probe at a distance of 0.5 nm with a voltage signal depicted in Fig. 5 formed a hysteresis loop. Typical I – V characteristics averaged over eight measurements are shown in Fig. 5. The shape of the I – V curves suggests the existence of the memristor effect in the structure based on the VA CNT array. The ratio R_{LR}/R_{HR} of the resistances in the low- and high-resistance states for the VA CNT array under investigation at a voltage of 180 mV amounts to 28. No hysteresis was observed on the I – V curves obtained at the lateral walls of the VA CNT bundle. The mechanism of the emergence of the memristor effect in the VA CNTs is obviously complex by nature and is probably associated with the polarization of the nanotube itself and with the formation of space charges at the tip of the STM probe.

Analysis of the memristor effect on various VA CNT bundles has shown that the ratio of the resistances in the low-resistance and high-resistance states depends on the geometrical parameters of bundles. Figure 6 shows the values of R_{LR} and R_{HR} for $U = 180$ mV for different VA CNT bundles (see Fig. 3c), which indi-

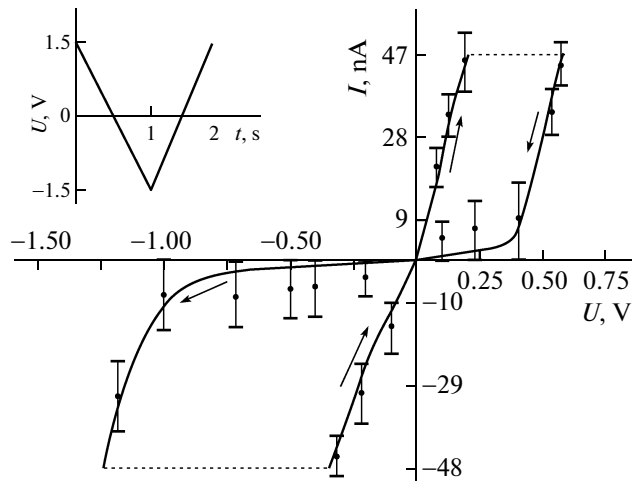


Fig. 5. I – V characteristics of VA CNT bundles (see Fig. 3c), obtained by the STM method. The inset shows the shape of the voltage signal fed per measuring cycle.

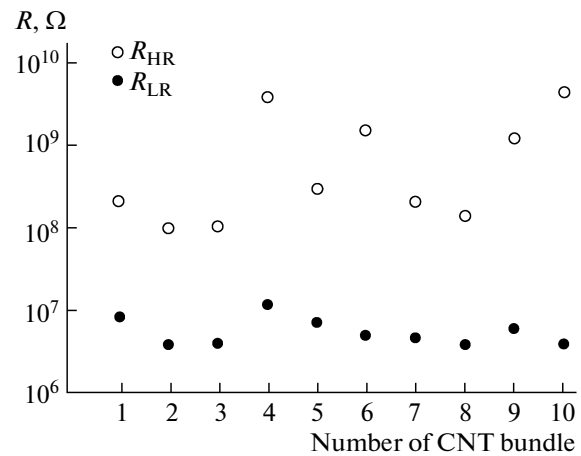


Fig. 6. Resistance R_{LR} and R_{HR} in the low-resistance and high-resistance states for different VA CNT bundles.

cate that the value of R_{HR} may change by almost two orders of magnitude depending on the geometrical parameters of the VA CNT bundle, while the value of R_{LR} changes by less than an order of magnitude.

Thus, when the vertices of VA CNT bundles are investigated using STM spectroscopy, the memristor effect depending on the geometrical parameters of VA CNT bundles is observed. Additional experiments are required for explaining the mechanism of the emergence of this effect.

CONCLUSIONS

We have studied the features of interaction of an STM probe with the surface of the VA CNT array experimentally using STM method. It is shown that when an external electric field is applied, individual

VA CNTs are combined into bundles with diameters determined by the radius of the STM probe tip and independent of the polarity of the applied voltage. This effect must be taken into account in analysis of the properties of VA CNTs by the STM method.

Analysis of the VA CNT array by the STM-spectroscopy reveals the existence of the memristor effect. The VA CNT bundles can be in the low-resistance or high-resistance state depending on the applied voltage, which can be associated with polarization of carbon nanotubes and the formation of a space charge at the tip of the STM probe. The ratio of resistances in the low- and high-resistance states of the VA CNT array was 28 at a voltage of 180 mV. It is shown that the values of resistances R_{LR} and R_{HR} may change by almost two orders of magnitude depending on the geometrical parameters of the VA CNT bundle.

Our results can be used in the development of technological processes for preparing energy-effective ultrahigh-access memory cells based on VA CNT arrays for elements of vacuum microelectronics and in analysis of geometrical and electrical properties of VA CNT by scanning probe microscopy.

ACKNOWLEDGMENTS

This work was supported by the Russian Foundation for Basic Research and the Federal Target Program “Human Capital for Science and Education in Innovative Russia” for 2009–2013 (contract nos. 14.A18.21.0900 and 12-08-90045/12).

REFERENCES

1. B. Bhushan, *Springer Handbook of Nanotechnology*, 3rd ed. (Springer, New York, 2010), p. 1964.
2. D. B. Strukov, G. S. Snider, D. R. Stewart, and R. S. Williams, *Nature* **453** (7191), 80 (2008).
3. L. Chua, *Appl. Phys. A: Mater. Sci. Process.* **102**, 765 (2011).
4. O. A. Ageev, O. I. Il'in, V. S. Klimin, B. G. Konoplev, and A. A. Fedotov, *Khim. Fiz. Mezoskop.* **13**, 226 (2011).
5. O. A. Ageev, O. I. Il'in, V. S. Klimin, A. S. Kolomiitsev, and A. A. Fedotov, *Izv. Yuzhnogo Fed. Univ., Tekh. Nauki*, No. 4, 69 (2011).
6. J. Yao, J. Zhong, L. Zhong, D. Natelson, and J. M. Tour, *J. Am. Chem. Soc.* **3**, 4122 (2009).
7. A. Radoi, M. Dragoman, and D. Dragoman, *Appl. Phys. Lett.* **99**, 093102 (2011).
8. K. Ichimura, M. Osawa, and K. Nomura, *Physica B* **323**, 230 (2002).
9. V. Meunier and Ph. Lambin, *Carbon* **38**, 1729 (2000).
10. O. A. Ageev, O. I. Il'in, A. S. Kolomiitsev, B. G. Konoplev, M. V. Rubashkina, V. A. Smirnov, and A. A. Fedotov, *Russ. Nanotekh.* **7**, 54 (2012).
11. O. A. Ageev, O. I. Il'in, A. S. Kolomiitsev, B. G. Konoplev, M. V. Rubashkina, V. A. Smirnov, and A. A. Fedotov, *Mikronanosist. Tekh.*, No. 3, 9 (2012).
12. A. Mayer, *Phys. Rev. B* **71**, 235333 (2005).
13. W. Lu, D. Wang, and L. Chen, *Nano Lett.* **7**, 2729 (2007).
14. G. S. Bocharov, A. A. Knizhnik, A. V. Eletsii, and T. J. Sommerer, *Tech. Phys.* **57**, 270 (2012).

Translated by N. Wadhwa